This paper describes objective technical results and analysis. Any subjective views or opinions that might be expressed in the paper do not necessarily represent the views of the U.S. Department of Energy or the United States Government.

SAND2018-3684C

Initial Closed-Loop Testing Results for the Pacific DC Intertie Wide Area Damping Controller

Daniel Trudnowski
Montana Tech
Butte, MT USA
dtrudnowski@mtech.edu

Brian Pierre, Felipe Wilches-Bernal, David Schoenwald, Ryan Elliott, Jason Neely, Raymond Byrne
Sandia National Laboratory
Albuquerque, NM USA

Dmitry Kosterev
Bonneville Power Administration
Portland, OR USA
dnkosterev@bpa.gov

***Abstract*—Lightly damped electromechanical oscillations are a source of concern in the western interconnect. Recent development of a reliable real-time wide-area measurement system (WAMS) has enabled the potential for large-scale damping control approaches for stabilizing critical oscillation modes. A recent research project has focused on the development of a prototype feedback modulation controller for the Pacific DC Intertie (PDCI) aimed at stabilizing such modes. The damping controller utilizes real-time WAMS signals to form a modulation command for the DC power on the PDCI. This paper summarizes results from the first actual-system closed-loop tests. Results demonstrate desirable performance and improved modal damping consistent with previous model studies.**

***Index Terms*—Power system oscillation control; Wide Area Measurement Systems; HVDC modulation.**

I. Nomenclature

BC	British Columbia, Canada.
BPA	Bonneville Power Administration.
COI	California-Oregon intertie.
MSF	multi-sine function.
PDCI	pacific DC intertie.
PMU	phasor measurement unit.
WAMS	wide area measurement system.
WI	western interconnect (the western North American power system).

II. Introduction

The WI has several inter-area modes due to long transmission paths and oscillatory instability was a contributing factor to the 1996 system break up [1]. Increased power transmission requests, increased penetration of renewable energy systems, low damping events observed in planning models, and increased observation of actual-system low-damping conditions have spurred engineering and research into the mitigation of such problems. The scope of actions includes implementation of a PMU-based real-time WAMS and the evaluation of large-scale oscillation damping devices/controls. This paper presents the initial actual-system results of a prototype DC modulation damping controller that utilizes WAMS feedback.

This work was supported by the BPA Technology Innovation Office and the Transmission Reliability and Energy Storage programs in the US Department of Energy Office of Electricity. Sandia National Laboratories is a multi-mission laboratory managed and operated by Sandia Corporation, a wholly owned subsidiary of Lockheed Martin Corporation, for the U.S. Department of Energy's National Nuclear Security Administration, under contract DE-AC04-94AL85000.

Fig. 1 shows a simplified one-line diagram of a reduced-order model of the WI taken from [2]. The PDCI is an 846-mile 3,200-MW DC transmission line connecting northern Oregon and southern California. The converter controls allow for modulation of the DC power on the line.

Experiments dating back to the 1970s [3] have shown that PDCI modulation has considerable potential for improving oscillatory stability. The approach used in [3] was based upon local-signal feedback. Although it improved damping of the desired mode, it destabilized a different mode [2].

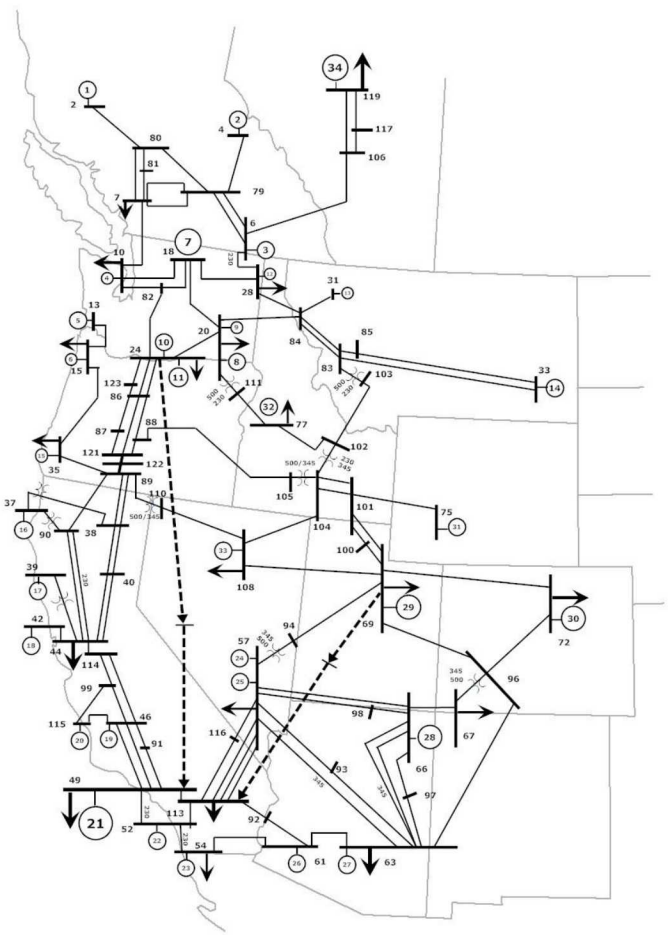

Fig. 1: Simplified one-line of WI.

The control strategy now being considered is described in [2] and relies upon WAMS feedback. Effectively, the DC modulation is proportional to the difference in frequency be-

Sandia National Laboratories is a multimission laboratory managed and operated by National Technology & Engineering Solutions of Sandia, LLC, a wholly owned subsidiary of Honeywell International Inc., for the U.S. Department of Energy's National Nuclear Security Administration under contract DE-NA0003525.

tween two geographically separated locations. Using transient-stability simulation and eigenanalysis, it is demonstrated in [2] that this approach has significant advantages over other approaches.

In addition to the model studies, nearly 100 open-loop actual-system modulation tests have been conducted since 2009 [4], [5]. These open-loop tests have confirmed and refined the model-based findings and provided critical information for fine-tuning the control algorithm.

In September of 2016, the first actual-system closed-loop tests were conducted. These tests included inducing transients into the WI and observing the performance of the damping controller over several days of operation. Initial analysis results from these tests are summarized in this paper.

III. WI Modes

This section provides a summary of the key inter-area modes of the WI and their properties. This topic is covered in greater detail in [2] and [4]. Based upon 30 years of actual-system testing and model studies, the frequency, damping, shape, observability, and controllability of the major inter-area modes are well known. The inter-area modes of interest are:

- "NSA Mode" nominally near 0.2 to 0.25 Hz;
- "NSB Mode" nominally near 0.35 to 0.4 Hz;
- "EWA Mode" nominally near 0.4 to 0.5 Hz;
- "BC" mode nominally near 0.6 Hz; and,
- "Montana" mode nominally near 0.8 Hz.

Other modes exist in the system; but, these five have been observed the most. Of the five modes, NSB is the most widespread and troublesome.

The NSA mode has the northern half of the system (Canada and the pacific northwest-US) swinging against the southern half (desert southwest US and southern California). The majority of power swings travel through the western path with the mode-shape dividing line typically near the COI. By far, the dominant observability and controllability point is in Alberta Canada. The PDCI has little controllability of this mode.

The NSB Mode first showed up after Alberta interconnected to the system and has a very widespread shape. It has the Alberta area swinging against BC and the northern US which in turn swings against the southern part of the US. The mode dividing line is typically near the COI. The observability/controllability is very widespread with no one location dominant. It is a very widespread mode. The PDCI has excellent controllability of the NSB mode.

Historically, the Alberta interconnection has the strongest influence on the NSA and NSB modes. With Alberta connected, the NSB mode typically has the lowest damping and is the most widespread and troublesome. Its damping is influenced by flows from Canada to California, which are historically high during the summer season. With Alberta disconnected, the two modes meld into a single north-south mode nominally near 0.32 Hz which again has a dividing line near the COI. This mode is typically lightly damped.

The EWA mode has the eastern part of the system, led by the Colorado area, swinging against the southwest. Model studies indicate the mode is controllable from generators in the Colorado area. The "BC" mode primarily has the BC area swinging against the rest of the system. The "Montana" mode has Montana oscillating against the rest of the system. Although these two modes are more localized, they do ripple through the system at a high enough energy to cause concern.

IV. Control Strategy

Fig. 2 shows the damping controller diagram based upon the control strategy described in [2]. Phasor voltages are measured from two locations within the AC system. V_L denotes the voltage at a *local* location near the north end of the PDCI; V_R denotes a *remote* location near the COI. A derivative filter, $H(z)$, computes a frequency measurement from the phasor angles reported by each PMU. The relative frequency Δf between the two locations is then calculated. Finally, a control gain K is applied to Δf to obtain the modulation command (in units of MW).

The guiding principles for the design of the control law of modulating PDCI power based upon the relative frequency error are:

- The law shall provide damping to any/all controllable modes that may occur in any AC system configuration.
- The law must not interact with frequency regulation of the overall system.

Hundreds of simulations, linear analyses, and actual-system probing tests have shown that the control law fulfills these two principles [2], [4], [5]. The concluding results of these past studies and tests are: 1) verification that the control strategy performs as desired; 2) optimal derivative filter settings; 3) requirements on the PDCI dynamics and the communication network delay; 4) desired PMU locations; and 5) selection of a range of control gains K.

Switch S_w in Fig. 2 is used to switch the damping controller in and out of closed-loop operation. The modulation signal is limited by the P_{max} saturation. Probing signals p_1 and p_2 are used to excite the system for testing purposes. P_0 is the PDCI set point. More details on the controller implementation are contained in [6].

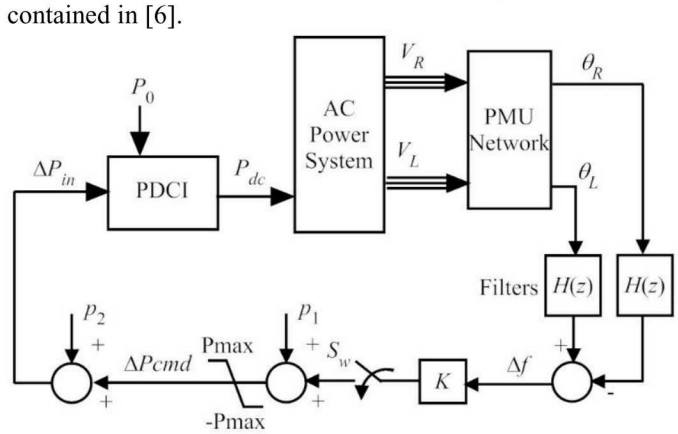

Fig. 2: Damping controller block diagram.

V. Test Objectives and Procedure

A series of open-loop and closed-loop actual-system PDCI control tests were conducted over several weeks in September 2016. These constitute the first actual-system closed-loop tests.

The tests described in this paper differ from pasts tests in two ways. First, a significant PDCI upgrade was completed at the end of 2015 [10]. This included replacement and updating of all converter components ranging from power-electronic apparatuses to transformers. An expected benefit of this upgrade is a faster and more accurate response to power commands such as modulation control. The second unique quality of the tests is that the damping controller prototype is fully developed and installed. All past probing tests had the ability to analyze the transfer function of the "AC Power System" component in Fig. 2 but not the "PDCI" dynamics.

A. Test Objectives

With these two characteristics in mind, the primary test objectives are to:

- characterize the PDCI dynamics;
- verify that the Fig. 2 "AC Power System" dynamics are consistent with past tests;
- demonstration and testing of the controller; and
- quantify the impact on system modes.

B. Test Procedure

Tests consisted of injecting probing signals into the control loop and exciting a large WI transients using the Chief Joseph Brake (CJB) [11] pulses. Tests were conducted both in open-loop and closed-loop. In general, tests can be split into three categories: calibration; MSF; and CJB pulses.

Calibration tests consist of applying simple probing signals (sine waves, square-wave pulses) into Fig. 2 via p_1 or p_2. The goals are to calibrate control settings, verify reasonable responses, and produce comparative data for other tests.

The MSF probing signal has frequency content from 0.02 Hz through 10 Hz. It consists of either 6 or 12 cycles of a 100-sec. signal and is scaled to $\pm$20 MW. It is the same MSF signal as used in past open-loop tests ([2], [4]). These tests are used to estimate a variety of transfer function properties. Spectral analysis via Welch's periodogram averaging [8] is used to estimate key transfer functions.

The CJB is a 1400 MW resistive brake located in Washington [11]. It is energized for a half second to initiate a large oscillatory transient in the WI. For this project, the brake was energized twice within a few minutes. Once with the system in open loop and then again with the system in closed loop. Because the pulses were initiated within a few minutes of each other, it is safe to assume the modal characteristics of the system had not changed. Ringdown analysis [9] is then used to estimate the modal frequencies and damping and to compare the closed-loop with the open-loop responses.

VI. PDCI Dynamics

Fig. 3 shows the estimated open-loop transfer function from ΔP_{in} to P_{dc} in Fig. 2 based upon 4 different MSF probing tests. This is the transfer function of the PDCI. The output P_{dc} is the real power measured from the PDCI on the AC side of the converter and is the actual power injected into the AC system. Each test is represented with a different color. The PDCI step response is shown in Fig. 4. The results in these figures (and the many more collected during the tests) show several ideal properties.

First, as reflected in Fig. 3, the gain of the PDCI is nearly flat with a bandwidth of nearly 7 Hz which is well past the dynamic bandwidth of electromechanical oscillations. The gain does increase slightly near 5 Hz indicating a slight under-damped response which is consistent with the step response in Fig. 4. Because this under-damped response is much faster than the expected modal oscillations, it is of minimal concern.

Second, the response time is very fast. The response of the PDCI is calculated from the slope of the phase in Fig. 3. In the control band (0.1 Hz to 1.0 Hz), the delay is approximately 11 msec. This is certainly within the limitations ([2], [4]).

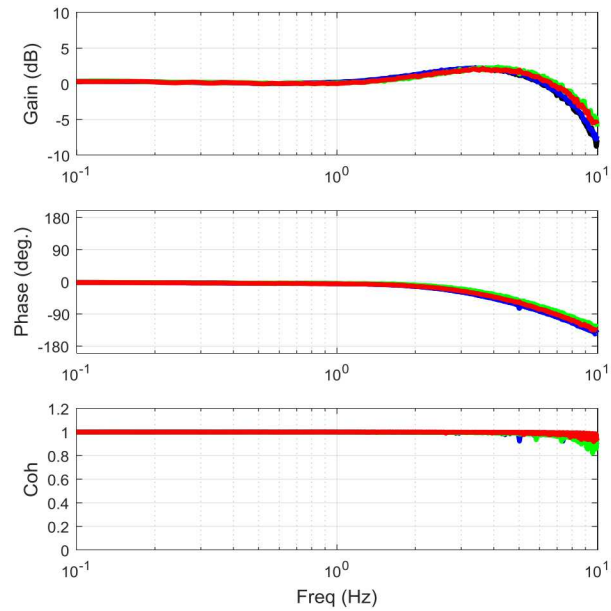

Fig. 3: Estimated PDCI transfer function for 4 different independent tests over a range of two weeks. Subplot 1 is the gain of the transfer function, subplot 2 is the transfer-function phase, and subplot 3 is the coherency between the input and output.

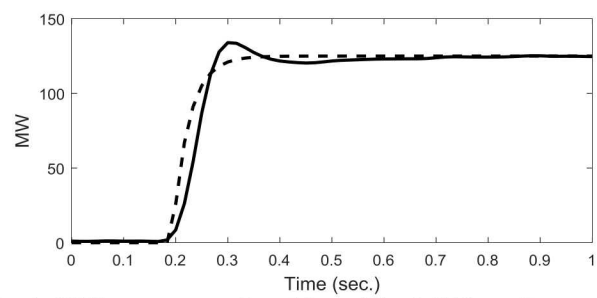

Fig. 4: PDCI step response. Dotted line = ΔP_{in}. Solid line = P_{dc}.

Thirdly, the system is not corrupted by noise. This is confirmed in the bottom subplot in Fig. 3 labeled "Coh" which shows the coherency between ΔP_{in} and P_{dc}. The coherency is a measure of correlation between two signals; a coherence of zero indicates no correlation and a coherence of unity indicates 100% correlation [8]. This plot demonstrates that nearly 100% of the modulation passes to the AC system.

Lastly, the response is very consistent. This is expected as the dynamics are governed by the PDCI converter controls and electronics which are certainly predicable.

VII. Loop Transfer Function

Fig. 5 shows the estimated open-loop transfer function of the entire loop for the four probing tests using a control gain K of 9MW/mHz. Note that an extra negative sign is included in the calculation in order to center the phase plot around 0°. It represents the transfer function from P_{dc} to $-\Delta P_{cmd}$ in Fig. 2. The results are very consistent with all the past probing tests described in [2], [4] and [5] and indicate improved damping for all modes controllable during the tests.

Peaks in the gain indicate a system mode below 1 Hz. The plots show three primary peaks near 0.25 Hz (NSA mode), 0.35 Hz (NSB mode), and 0.7 Hz (BC mode). As typical of the WI, the modal properties change depending on the particular operating conditions. The dynamics above 1 Hz are primarily due to the PDCI physics.

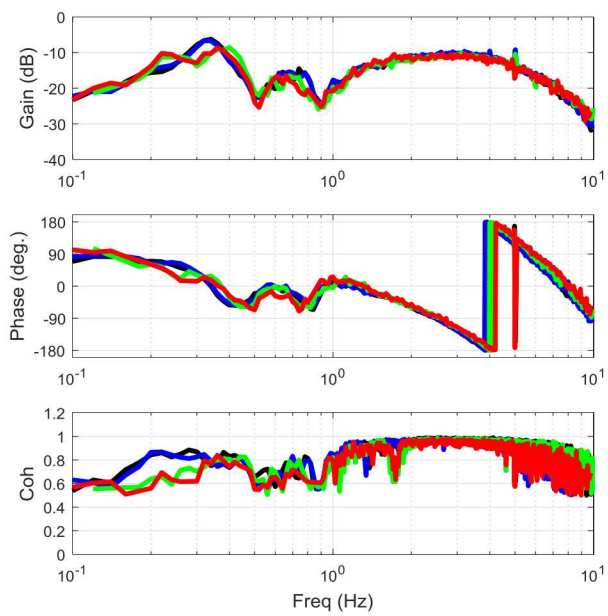

Fig. 5: Estimated loop transfer function for 4 different independent tests over a range of two weeks and a gain of 9 MW/mHz. Subplot 1 is the gain of the transfer function, subplot 2 is the transfer-function phase, and subplot 3 is the coherency between the input and output.

Damping is added to a given mode if the phase is transitioning through 0° near the peak frequency of the mode ([2], [4]). If the phase is outside ±90°, the controller will destabilize the mode. Damping is added to all modes for all four tests. This is consistent with the nearly 100 tests conducted since 2009 ([4], [5]).

A gain of 9 MW/mHz assures a gain margin of 10 dB at a cross over frequency of 4 Hz. This represents good robustness properties. The 4 Hz crossover is well outside the range of electromechanical mode frequencies. A gain margin of 6 dB equates to a gain of 14.2 MW/mHz which represents the maximum prudent gain in terms of stability with this feedback configuration.

VIII. Closed Loop Response

A variety of closed-loop versus open-loop responses were collected to evaluate the effectiveness of the controller in damping oscillations. In all cases oscillation damping was improved consistent with model studies.

Fig. 6 compares the responses to 3 cycles of a ±125-MW 2.5-sec. pulse train applied at p_2 in Fig. 2. This test is a good low-amplitude qualitative evaluation for the controller. As seen in the plot, the controller is clearly adding damping to the oscillation. Many more similar low-level tests were conducted with all indicating similar performance.

Pulsing the CJB is a more significant test. Fig. 7 shows the feedback signal from the AC system for back-to-back brake pulses. In one case, the system is in open loop while in the other it is in closed loop with a gain of 9 MW/mHz. The corresponding commanded P_{dc} is shown in Fig. 8. The controller clearly improves the damping.

Results for the gain increased to 12 MW/mHz are shown in Fig. 9 and Fig. 10. Again, the improved damping is very clear and slightly more than the K = 9 MW/mHz case. In this case, the controller reaches saturation during the 1st swing. Also note the increased noise in P_{dc} in Fig. 10. This noise is caused by the ambient conditions from the feedback signal. Future work will focus on using a smooth dead zone in the feedback to suppress this noise.

Table 1 compares the open-loop and closed-loop NSB mode properties. The properties were estimated via ringdown analysis [9]. In closed loop, the mode damping is improved in the 4% to 5% range which is considerable. Other modes also showed improved damping but were harder to quantify as their initial damping was very high. The improved damping is consistent with previous model studies [2]; but, more analysis is required as those studies were typically conducted under much lower damping conditions

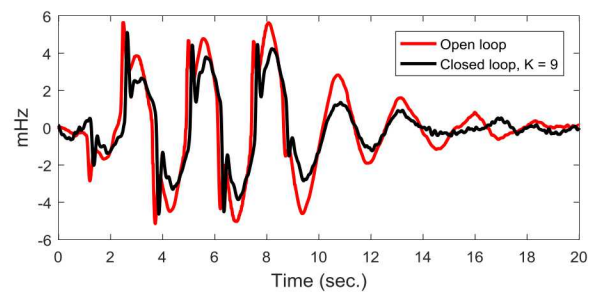

Fig. 6: Δf responses to a pulse train prove. Open loop versus closed loop with K = 9 MW/mHz and P_{max} = 125 MW (per Fig. 2).

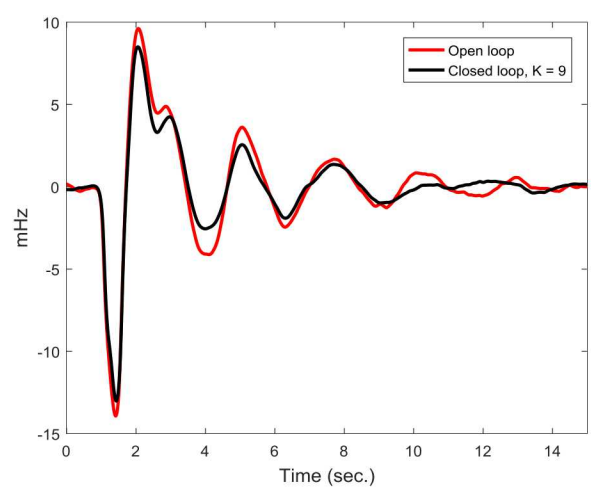

Fig. 7: Δf responses for back-to-back CJB brake pulses. Open loop versus closed loop with K = 9 MW/mHz and P_{max} = 125 MW (per Fig. 2).

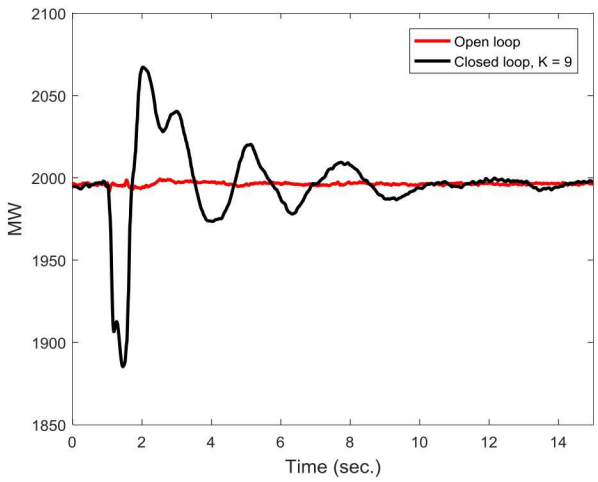

Fig. 8: P_{dc} for the cases in Fig. 7.

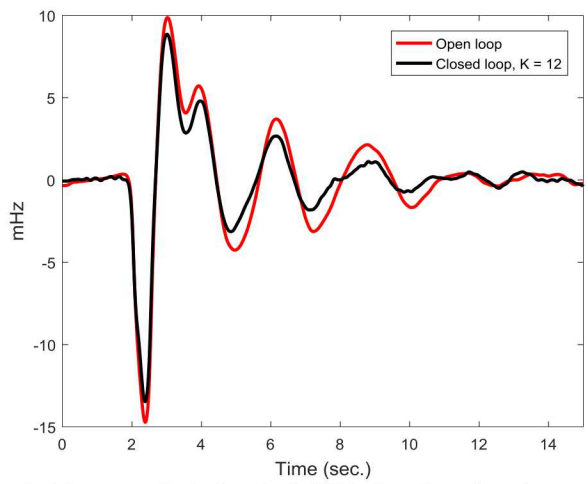

Fig. 9: Δf responses for back-to-back CJB brake pulses. Open loop versus closed loop with K = 12 MW/mHz and P_{max} = 125 MW (per Fig. 2).

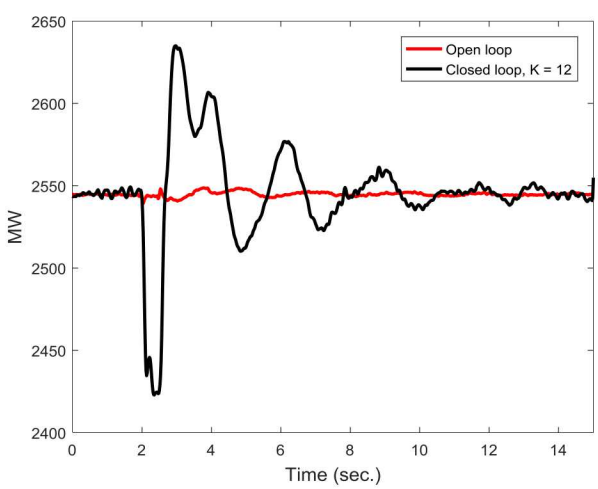

Fig. 10: : P_{dc} for the cases in Fig. 9.

Table 1: NSB mode estimates from four CJB pulse responses.

K	Open Loop		Closed Loop	
(MW/mHz)	Freq (Hz)	D (%)	Freq (Hz)	D (%)
9	0.383	11.7	0.364	16.1
12	0.390	12.7	0.385	17.8

IX. Conclusions

This paper describes the initial actual-system test results for a damping controller that modulates the PDCI based upon WAMS feedback. It represents the culmination of many years of testing and planning. Key findings in this paper include:

- The PDCI dynamics have excellent modulation control properties. This includes excellent dynamic response and noise rejection.
- Using north-to-COI feedback signal at a gain in the 9 to 12 MW/mHz range provided on the order of 4% to 5% damping to the critical NSB mode. It also increased the damping of other modes.
- At a gain of 9 MW/mHz, the control loop has a margin of 10 dB with a cross-over of 4 Hz which are excellent robustness properties.

Future research will center around further testing and refinement of the controller. This includes testing under lighter damping and higher stressed system conditions, introducing a dead zone to reduce noise, and under stressed voltage conditions near the PDCI. Also, future tests will be used to fully exercise all the supervisory conditions described in [6]. Lastly, more detailed analysis of these tests shall be performed including more detailed simulation comparisons.

X. Acknowledgment

The authors gratefully acknowledge the contributions of the those who enabled the system tests described in this paper. The tests were made possible by the expertise and contributions of BPA engineers Mr. Michael Overeem, Mr. Greg Stultz, and Mr. Daniel Goodrich.

XI. References

[1] D. Kosterev, C. Taylor, and W. Mittelstadt, "Model validation for the August 10, 1996 WSCC system outage," *IEEE Trans. On Power Systems*, vol. 14, no. 3, pp. 967-976, Aug. 1999.

[2] D. Trudnowski, D. Kosterev, and J. Undrill, "PDCI damping control analysis for the western North American power system," *IEEE PES General Meeting*, Vancouver BC, July 2013.

[3] R. Cresap, W. Mittelstadt, D. Scott, and C. Taylor, "Operating experience with modulation of the Pacific HVDC intertie," *IEEE Trans. on Power Apparatus and Systems*, vol. PAS-97, no. 4, pp. 1053-1059, July/Aug. 1978.

[4] D. Trudnowski, D. Kosterev, and J. Wold, "Open-loop PDCI probing tests for the wester north American power system," *IEEE PES General Meeting*, July 2014.

[5] D. Trudnowski, "2014 Probing Test Analysis," TIP 289 project report to BPA, Jan. 2014.

[6] B. Pierre, R. Elliott, D. Schoenwald, J. Neely, R. Byrne, D. Trudnowski, and J. Colwell, "Supervisory system for a wide area damping controller using PDCI modulation and real-time PMU feedback," *IEEE PES General Meeting*, July 2016.

[7] J. Pierre, N. Zhou, F. Tuffner, J. Hauer, D. Trudnowski, and W. Mittelstadt, "Probing signal design for power system identification," *IEEE Trans. on Power Systems*, vol. 25, no. 2, pp. 835-843, May 2010.

[8] J. Bendat and A. Piersol, Engineering Applications of Correlation and Spectral Analysis, 2nd Ed., John Wiley & Sons, Inc., 1993.

[9] D. Trudnowski and J. Pierre, "Signal Processing Methods for Estimating Small-Signal Dynamic Properties from Measured Responses," Chapter 1 of Inter-area Oscillations in Power Systems: A Nonlinear and Nonstationary Perspective, ISBN: 978-0-387-89529-1, Springer, 2009.

[10] K. Wingert, "BPA puts modernized Celilo Converter Station into service," BPA News Release, PR 03-16, Jan. 2016.

[11] M. Shelton, W. Mittelstadt, P. Winkelman, W. Bellerby, "Bonneville Power Administration 1400—MW braking resistor," *IEEE Trans. on Power Apparatus and Systems*, vol. 94, no. 2, pp. 602-611, March 1975.